BIOCHEMISTRY
including biophysical chemistry & molecular biology

Article

pubs.acs.org/biochemistry

Mycobacterium tuberculosis NmtR Harbors a Nickel Sensing Site with Parallels to *Escherichia coli* RcnR

Hermes Reyes-Caballero,[†,‡] Chul Won Lee,[†] and David P. Giedroc*[,†]

[†]Department of Chemistry, Indiana University, Bloomington, Indiana 47405-7102, United States

[‡]Department of Biochemistry and Biophysics, Texas A&M University, College Station, Texas 77843-2128, United States

Supporting Information

ABSTRACT: *Mycobacterium tuberculosis* NmtR is a Ni(II)/Co(II)-sensing metalloregulatory protein from the extensively studied ArsR/SmtB family. Two Ni(II) ions bind to the NmtR dimer to form octahedral coordination complexes with the following stepwise binding affinities: $K_{Ni1} = (1.2 \pm 0.1) \times 10^{10}$ M^{-1}, and $K_{Ni2} = (0.7 \pm 0.4) \times 10^{10}$ M^{-1} (pH 7.0). A glutamine scanning mutagenesis approach reveals that Asp91, His93, His104, and His107, all contained within the C-terminal α5 helix, and His3 as part of the conserved α-NH_2-Gly2-His3-Gly4 motif at the N-terminus make significant contributions to the magnitude of K_{Ni}. In contrast, substitution of residues from the C-terminal region, His109, Asp114, and His116, previously implicated in Ni(II) binding and metalloregulation in cells, gives rise to wild-type K_{Ni} and Ni(II)-dependent allosteric coupling free energies. Interestingly, deletion of residues 112−120 from the C-terminal region (Δ111 NmtR) reduces the Ni(II) binding stoichiometry to one per dimer and greatly reduces Ni(II) responsiveness. H3Q and Δ111 NmtRs also show clear perturbations in the rank order of metal responsiveness to Ni(II), Co(II), and Zn(II) that is distinct from that of wild-type NmtR. ^{15}N relaxation experiments with apo-NmtR reveal that both N-terminal (residues 2−14) and C- terminal (residues 110−120) regions are unstructured in solution, and this property likely dictates the metal specificity profile characteristic of the Ni(II) sensor NmtR relative to other ArsR family regulators.

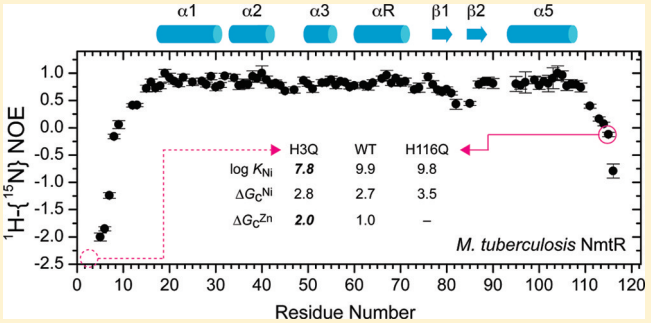

The genome of the human pathogen *Mycobacterium tuberculosis* (*Mtb*)[1] encodes an impressive diversity of known and putative metal ion transporters, including 12 putative P-ATPases and several ABC transporters and cation diffusion facilitator (CDF) transporters.[2] This diversity might have allowed a primordial soil-dwelling ancestor of *Mtb* to adapt to an environment of substrate complexity.[1] At present, this diversity might allow this obligate intracellular pathogen to efficiently respond to a range of host-killing mechanisms,[3] collectively known as nutritional immunity.[4,5]

A limited number of enzymes are known that require nickel as a cofactor.[6,7] *Mtb* encodes a urease (Rv1848), as well as a gene encoding a hypothetical Ni(II)-containing glyoxylase I (Rv0546c) that metabolizes the electrophile methylglyoxal.[8] In *Mycobacterium bovis* BCG, thought to be a progenitor strain of *Mtb*,[9] the catalytic product of urease, ammonia, is believed to be important in host survival as it neutralizes the pH of the phagosome, inhibits lysosome−phagosome fusion, attenuates the exposure of the major histocompatibility complex class II in the host cell surface, and is used for nitrogen biosynthesis.[10−12] Because *Mtb* does not compete against its host for nickel acquisition,[13−16] in contrast with other essential metals in humans, including Fe,[17,18] this urease-dependent function may represent an important pathogenesis determinant in *Mtb*. As a result, *Mtb* is predicted to encode complete Ni uptake and Ni efflux systems. Although the importance of Ni homeostasis in *Mtb* pathogenesis remains poorly understood, it has been reported that total nickel levels as measured by X-ray fluorescence microscopy fall precipitously inside macrophages infected with *Mtb*.[19,20]

Nickel specific transcriptional regulation of genes encoding uptake, efflux, detoxification, sequestration, and regulatory proteins[21] may well be required for adaptation and survival of *Mtb* in the human host. Some metalloregulators, transcriptional regulators that are activated or inhibited to bind DNA in response to a metal, encoded by the *Mtb* genome have been previously characterized (Table S1 of the Supporting Information). There are two Ni(II) specific repressors in mycobacteria, and both are members of the ArsR/SmtB family of metal sensors, of 10 total ArsR family regulators encoded by *M. tuberculosis*.[21−23] These are NmtR and KmtR, which repress the transcription of *ctpJ* and *cdf*, encoding a P-type ATPase metal transporter and a putative cation diffusion facilitator (CDF) transporter, respectively, at low Ni(II) concentrations. At high Ni(II) concentrations, NmtR and KmtR bind Ni(II) and dissociate from the DNA, allowing transcription of *ctpJ* and

Received: May 12, 2011
Revised: August 6, 2011
Published: August 7, 2011

cdf, the gene products of which are predicted to mediate the export of Ni(II) and Co(II), respectively, from the cytoplasm.[2,24] In other organisms, complete Ni(II) homeostasis systems have been characterized. In *Escherichia coli*, *rcnA* encodes a Ni(II)/Co(II) efflux protein[25] whose expression is controlled by RcnR,[26,27] a member of a recently discovered CsoR/RcnR family of regulators,[26,28] while *nikABCDE* is a high-affinity ABC-type transporter that mediates acquisition of Ni(II) and is under the transcriptional control of NikR.[29−31] In the actinomycete closely related to *Mtb*, *Streptomyces coelicolor* Nur, a Fur family member, coordinates the expression of Ni(II) versus Fe(II) superoxide dismutase (*sodN* and *sodF*) and of *nikABCDE*.[32,33] The nickel uptake regulator in *Mtb* has not yet been identified or functionally characterized.

Several members of the ArsR family of metalloregulators have now been extensively studied. *Staphylococcus aureus* Zn(II) sensor CzrA is the best characterized family member with respect to its functional, structural, and thermodynamic mechanism of allosteric regulation.[34−36] A current hypothesis is that transition metal selectivity cell is dictated primarily by coordination geometry, and support for this model comes from comparative studies contrasting the metal center structures of two α5 site metalloregulators of the ArsR/SmtB family, NmtR, a Ni(II)/Co(II) sensor, and CzrA, a Zn(II)/Co(II) sensor (see Figure 1 for a schematic).[21] CzrA binds Zn(II) in a tetrahedral

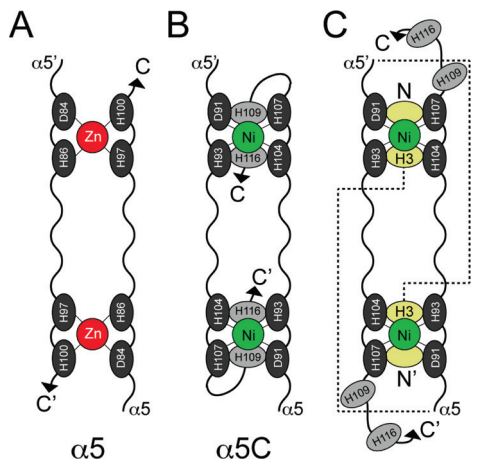

Figure 1. Schematic rendering of symmetry-related metal sensing sites in ArsR family protein dimers. (A) Canonical interprotomer tetrahedral Zn(II) sensing sites structurally characterized in *S. aureus* CzrA.[36] Only the C-terminal α5 helices of each protomer are shown, and ligand donor residues are indicated. (B) Previously proposed octahedral[37] Ni(II)/Co(II) sensing site of *M. tuberculosis* NmtR denoted α5C.[22] The C-terminal α5 helices and tail are shown as are proposed ligand donor residues. (C) Alternative Ni(II) sensing site in NmtR consistent with the experimental findings outlined here, with the region N-terminal to the α5 helices (residues 2−91) simply represented as a dashed line. It is unknown if coordination of Ni(II) by His3 is intra- or interprotomer relative to His104/His107; intraprotomer coordination is shown. The identity of the sixth ligand (empty tan oval) is not given here, but a strong candidate is the α-amino group of Gly2 (see the text for details).

geometry via ligands derived from the C-terminal α5 helix and thus is designated an α5 site. NmtR binds Ni(II) and Co(II) with octahedral coordination that is proposed to include the analogous core of four CzrA zinc ligands supplemented with an additional two ligands from the C-terminus (designated α5C) to complete the six-coordinate complex (Figure 1).[37] These metal coordination geometries correspond to the most common coordination geometries found for Ni(II) and Zn(II) in proteins.[38] The binding of the noncognate metal to NmtR or CzrA results in formation of a non-native coordination geometry that gives rise to greatly attenuated or eliminated metalloregulation of DNA binding.[37] A residue substitution mutagenesis screen of CzrA revealed that two metal ligands were necessary to maintain the native coordination geometry and Zn(II)-mediated regulation [D84 and H97 (Figure 1A)], while two other ligands were necessary only for maintaining high metal affinity with no or small effects on regulation [H86 and H100 (Figure 1A)], in what was termed a "division of labor" organization.[39] As a result, it has been hypothesized that the metal coordination geometry is a primary determinant of metal selectivity for metalloregulators,[40,41] and this hypothesis is supported by accumulating evidence from multiple families of metalloregulators, including CsoR and NikR.[42]

A previous in vivo study of NmtR identified functionally important metal ligands in the α5 helix, D91, H93, H104, and H107, exactly coincident with the Zn(II) regulatory site of CzrA, as well as C-terminal residues H109 and H116[22] (see Figure 1B). In this study, we further tested this model by measuring the affinity of the nickel center and metal-mediated negative allosteric regulation of DNA binding of a panel of conservative glutamine substitution mutants, i.e., single H-to-Q and D-to-Q substitutions. These studies provide new insights into the specific contributions of the N- and C-terminal regions in NmtR relative to CzrA in maintaining Ni(II) selectivity and Ni(II)-mediated regulation in *Mtb*. In short, we provide evidence of an N-terminal Ni(II) binding interaction involving His3 like that described for the Ni(II)/Co(II) sensor *E. coli* RcnR (Figure 1C).[26] An as yet uncharacterized putative NmtR in *Streptomyces coelicolor* (locus tag SCO6459) also conserves the N-terminal Gly2-His3-Gly4 motif found in *Mtb* NmtR. In contrast, previously implicated Ni(II) ligands H109 and H116 are not conserved (Figure 2), and we show here that conservative substitution of each shows that neither plays an identifiable role in negative allosteric regulation of DNA binding of Ni(II) binding in vitro. The implications of these findings are discussed.

EXPERIMENTAL PROCEDURES

Protein Purification. Protein purification was essentially conducted as previously described.[22,37] This purification scheme involves PEI precipitation of lysis supernatant, followed by two successive ammonium sulfate cuts (35 and 70%) and dissolution in 25 mM MES buffer (pH 6.0), 0.1 M NaCl, and 5 mM EDTA in preparation for a SP (sulfopropyl)-Sepharose chromatography. Peak fractions were pooled and subjected to Q-Sepharose chromatography in 25 mM Tris (pH 8.0) and 0.05 M NaCl, with final polishing with a G75 preparative grade gel filtration run in 10 mM Hepes (pH 7.0) and 0.2 M NaCl buffer. The G75 elution volume of all the NmtR mutants is consistent with a dimer assembly state in all cases. All mutant NmtRs were shown by ESI-MS to give the expected molecular weight if one assumes that in all cases the N-terminal Met1 is processed (Table S2 of the Supporting Information) to yield an N-terminal α-NH_2-Gly2-His3-Gly4 sequence.

Anisotropy Experiments. These binding experiments and the purification of DNA were conducted as previously described.[43] The protein sample was diluted to a concentration of 10 μM, and 2−4 μL of this stock solution was titrated into 1800 μL of 10 nM dsDNA in 10 mM Hepes (pH 7.0) and 0.4

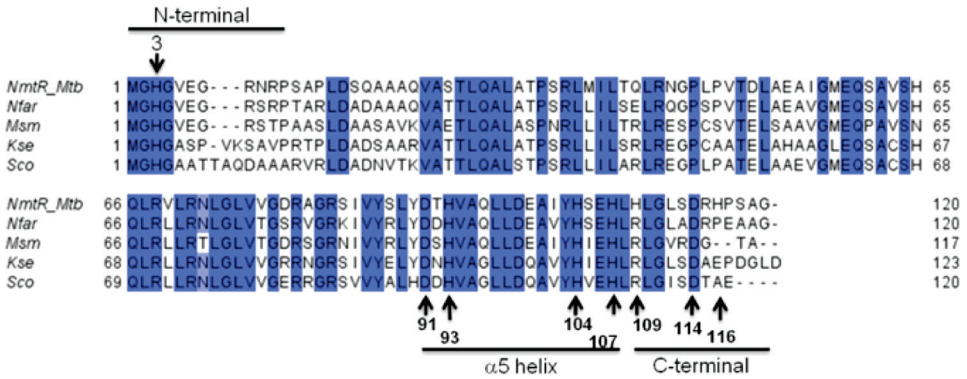

Figure 2. Multiple-sequence alignment of SmtB/ArsR family members that were obtained with NmtR as a query. The results were filtered by selecting those sequences that possess a C-terminal extension past residue 114 of NmtR. Conserved residues are highlighted in blue. Arrows indicate residues that were substituted with glutamines in this work, with NmtR numbering: Mtb (*Mtb*), locus tag Rv3744; Nfar (*Nocardia farcinica*), locus tag nfa31050; Msm (*Mycobacterium smegmatis*), locus tag MSMEG_5405; Kse (*Kitasataspora setae*), locus tag KSE_71210; Sco (*S. coelicolor*), locus tag SCO6459. All belong to phylum Actinobacteria.

M NaCl (unless otherwise noted) and allowed to equilibrate for 3−6 min. These binding reaction mixtures contained either 500 μM EDTA or 10 or 100 μM Ni(II), Co(II), or Zn(II) as indicated. The DNA sequence corresponds to the wild-type *nmt* operator containing the imperfect repeat known to be the binding site (underlined)[22] and is fluorescein (FL) labeled at the 3′ end (5′-GAAATAAA*TGAACA*TA*TGATCA*TA-TATTCT-3′-FL). For nonspecific DNA, 200 ng/mL DNA (sodium salt) from salmon testes (Sigma) was added to the buffer, diluted by stirring in a heating block at 60 °C for 6 h, and autoclaved. Anisotropy measurements have a standard error of ≤0.001 with the slit set to 1.0 for experiments at 0.2 M NaCl and to 2.0 for experiments at 0.4 M NaCl. The excitation monochromator was set to λ_{480}, instrument in L-format, long-pass filter λ_{515} in the emission and *G* factor set to 1. All the data were fit to the model described in the text using DynaFit.[44] The fit accounts for a dimerization constant of 1.9×10^5 M^{-1} ($K_{dimer,apo}$) or 4.1×10^5 M^{-1} ($K_{dimer,Ni}$).[37]

Tyrosine Fluorescence Experiments. Experiments were conducted as previously described.[22] In 1800 μL of 10 mM Hepes buffer (pH 7.0) at 25 °C and 0.2 M NaCl, wild-type NmtR and mutant variants were diluted to 5−10 μM and fluorescence was measured every *i*th addition of 1−4 μL of 0.5−2 mM $NiCl_2$, waiting 3 min after each addition to allow for equilibration. The excitation monochromator was set at λ_{260} and emission collected through the monochromator set at λ_{300}, with a 2.0 slit, with a mesh used at the emission channel when the high protein concentration is used. An average of 100 iterations for each addition was recorded. The chelator nitrilotriacetic acid (NTA) or *N*,*N*′-ethylene glycol tetraacetic acid (EGTA) was added to a final concentration of 18−21 μM from a concentrated stock solution calibrated by metal addition monitored by isothermal titration calorimetry. Metal stocks were quantified by atomic absorption as described previously.[22,37]

mag-fura 2 Competition Experiments. NmtR variants and competitor mag-fura 2 (mf2) were diluted in 1800 μL of buffer [25 mM Hepes (pH 7.0) and 0.2 M NaCl at 25 °C] to the concentration indicated in the text. Aliquots of 2 μL from a 0.5−1 μM Ni(II) stock were added to the mixture; the mixture was equilibrated for 3 min, and the excitation spectra (λ_{ex} = 377−383 nm, 0.5 slit) were recorded (λ_{em} = 497 nm, 1.0 slit) using the monochromator. An average of 30 iterations for every *i*th addition was recorded using an ISS PC1 instrument.

Co(II) Electronic Absorption Spectroscopy. These experiments were conducted as previously described for wild-type NmtR.[37] A sample of NmtR or NmtR variants was diluted in buffer [10 mM MES (pH 6.0) and 0.2 M NaCl at room temperature] and titrated with 2−10 μL of a 100 μM to 2 mM Co(II) stock solution, and the UV−visible spectra were recorded following every *i*th addition. The apoprotein spectra were subtracted and the resulting difference spectra corrected for dilution.

Calculation of NTA, EGTA, and mf2 Ni(II) Affinity Constants. EGTA-Ni(II) and NTA-Ni(II) affinity constants was calculated by the Schwarzenbach's α coefficient method (eqs 1−3)

$$\beta_n' = \beta_n/\alpha_M(\alpha_L)^n \quad (1)$$

$$\alpha_M = ([M] + [MOH] + [M(OH)_2] + ...)/[M] \quad (2)$$

$$\alpha_L = ([L] + [HL] + [H_2L] + ...)/[L] \quad (3)$$

and for the NTA-Ni(II) equilibria the NTA Ω factor was also used:

$$\Omega = 1 + \beta[NTA] + \beta_2[NTA]^2 \quad (4)$$

$$K' = \Omega K_{obs} \quad (5)$$

where K_{obs} is equal to the observed affinity while K' is the actual or corrected affinity of NmtR for Ni(II).

NMR Spectroscopy. NMR spectra were recorded at 37 °C on a Varian 600 spectrometer equipped with a cryogenic probe and were referenced to DSS. Protein samples were prepared in NMR buffer [10 mM Hepes (pH 7.0) and 100 mM NaCl] at a concentration of 0.5 mM. ^{13}C- and ^{15}N-labeled protein NMR data processing and analysis were performed using NMRPipe[45] and NMRView.[46] Sequence specific resonance assignments of the NmtR homodimer were obtained with uniformly ^{13}C- and ^{15}N-labeled NmtR using standard triple-resonance NMR spectroscopy: HNCA,[47] HN(CO)CA,[48] HNCACB,[49] and CBCA(CO)NH.[47]

RESULTS

Apo-NmtR Is Characterized by Flexible N-Terminal and C-Terminal "Tails". A multiple-sequence alignment of *Mtb* NmtR with other closely related ArsR/SmtB family sensors

with the highest degree of pairwise similarity to that of NmtR is shown in Figure 2. Although none of the other putative regulators have been characterized, this alignment reveals the Gly2-His3-Gly4 sequence and the previously characterized α5 site metal ligands Asp91, His93, His104, and His107 are invariant; in contrast, previously implicated regulatory Ni(II) ligands His109 and His116 are not. Asp114, not previously implicated in Ni(II) sensing in vivo, is in contrast conserved. Here, we evaluate the importance of each of these residues in Ni(II) binding and Ni(II) regulation in vitro by employing a Gln scanning mutagenesis approach.

Complete backbone assignments were obtained for residues 4−120 of apo-NmtR, with residues 2, 3, and 91−93 broadened beyond detection in this conformational state. The secondary structure of apo-NmtR was obtained from an analysis of the backbone chemical shifts using TALOS+,[50] and these data are shown superimposed on the primary structure in Figure 3. As

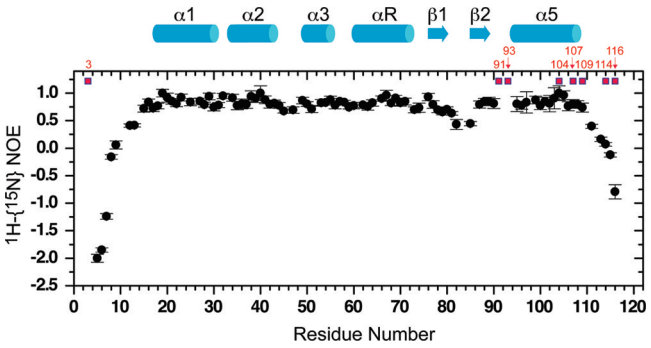

Figure 3. ^{1}H−{^{15}N} heteronuclear NOE (hNOE) of apo-NmtR. The hNOEs of two C-terminal residues (residues 119 and 120) are strongly negative (approximately −12) and are not shown for the sake of clarity. Secondary structural regions are α1 (17−30), α2 (33−43), α3 (49−55), α4 (αR) (60−72), β1 (76−80), β2 (85−88), and α5 [(94)−108] (because residues 91−93 are exchange broadened, the actual start of helix α5 is unknown). The residues targeted for substitution in this study are highlighted in red.

expected from previous solution and crystallographic structures of related ArsR/SmtB family sensors, NmtR has five helical segments (α1−α5) and two β-strands (β1 and β2) encompassing residues 17−108 arranged in an α1−α2−α3−α4 (αR)−β1−β2−α5 structure as expected for a winged helix protein. Residues 2−14 and 110−120 are highly mobile in solution, as revealed by chemical shifts at or near random coil values, and a value of the ^{1}H−{^{15}N} heteronuclear NOE that is weakly positive or negative (Figure 3). It is interesting to note that the extreme N-terminal residues 2−4 are strongly exchange broadened in the apo state (with His3 unassigned), in contrast to C-terminal residues.

Wild-Type NmtR Metal Binding Affinity. The metal ligands were functionally identified using intrinsic fluorescence as a reporter of metal binding. On a sequence alignment based on structural homologues, three tyrosine residues (Y87, Y90, and Y103) are predicted to flank the metal binding residues in NmtR (Figure 2).[21] Consistent with previous studies,[37] NmtR binds Ni(II) with a concomitant 30−35% increase in the intrinsic tyrosine fluorescence, with a stoichiometry of two Ni(II) mol equivalents per dimer or one per protomer (Figure 4A). Because this binding curve is essentially stoichiometric, only a lower limit of the Ni(II) binding affinity of $\geq 10^8$ M^{-1} could be obtained. Thus, a competitor chelator was included in the binding experiments to extract quantitative metal stability constants. The chelators nitrilotriacetic acid (NTA)[35] and *N*,*N*′-ethylene glycol tetraacetic acid (EGTA) were used for this purpose. The apparent stability of EGTA for Ni(II) corrected for the experimental pH used here (7.0) is 2.14×10^9 M^{-1} ($K_{EGTA\text{-}Ni}$) using the Schwarzenbach's α coefficient method[51] and pH-independent parameters taken from published NIST values.[52] The affinity of Ni(II) for NTA was calculated (see Experimental Procedures) using the Ω coefficient method ($\Omega = 1.56 \times 10^4$, pH 7.0, 20 μM NTA) or the Schwarzenbach's α coefficient ($\alpha_L = 4 \times 10^2$, $K_{NTA\text{-}Ni} = 6.01 \times 10^8$ M^{-1}, $\beta 2 = 7.7 \times 10^{13}$ M^{-2} at pH 7.0), with both methods giving similar results.

The Ni(II) binding isotherms measured in the presence of NTA and EGTA for wild-type NmtR are very similar, and each is indicative of an affinity for Ni(II) that is slightly higher than that of either competitor ligand (Figure 4B,C). On the basis of the binding stoichiometry of 1:1 (metal:monomer) (Figure 4A) and a dimeric assembly state [as determined by gel filtration in the micromolar range (see Experimental Procedures)], we chose a Ni(II) binding model of two stepwise metal binding events (K_{Ni1} and K_{Ni2}) on a nondissociable dimer to analyze these data. The results show that wild-type NmtR binds Ni(II) with an affinity of $\approx 10^{10}$ M^{-1} ($K_{Ni1} \approx K_{Ni2}$) (Figure 4B,C and Table 1). Interestingly, K_{Ni} is $\approx 10^4$ larger than the K_{Co} previously measured using the same approach.[22]

NmtR Is Allosterically Regulated by Ni(II) > Co(II) > Zn(II). NmtR binds to an intergenomic operator/promoter region in the absence of Ni(II) and represses the expression of a reporter gene in vivo.[22] Transcription is derepressed upon addition of Ni(II) or Co(II) to the growth medium, but not by the addition of Zn(II).[22] Here, we were interested in quantifying the metal affinity and allosteric response of NmtR to different metals and the extent to which single-substitution mutants influence this response. Ni(II) affinities are listed in Table 1 with DNA binding properties summarized in Table 2. We employed an anisotropy-based experiment to measure allosteric regulation using a 30 bp fluorescein-labeled duplex DNA that harbors the quasi-perfect inverted repeat sequence to which NmtR binds.[22]

To our surprise, Ni(II) was found to reduce the binding affinity by only ≈20-fold with respect to that of apo-NmtR versus the expected value of 200−300-fold observed previously at a higher monovalent salt concentration (0.4 M NaCl) (Table 2).[37] This finding suggested that Ni(II)-NmtR forms a DNA complex characterized by significant nonspecific binding interactions at 0.2 M NaCl. To test this, we measured the DNA binding affinity of NmtR for its operator at 0.4 M NaCl in the presence and absence of nonspecific DNA, in an effort to decrease the nonspecific electrostatic component of the interaction. We fit the anisotropy data to a dimer linkage model with the dimerization equilibrium constant fixed to the value previously measured.[37] In addition, the change in anisotropy that results from titrating apo-NmtR into the DNA probe (Δr_{mas}) is 0.016, consistent with previous stoichiometric determinations of binding of one dimer per DNA of similar length.[34,37,53] These data (Figure 5A and Table 2) reveal that apo-NmtR binds to DNA with a K_{DNA} of $(9.0 \pm 0.3) \times 10^9$ M^{-1} at 0.4 M NaCl in a manner independent of the presence of the competitor DNA; thus, this is the specific binding affinity of apo-NmtR for its operator sequence.

Addition of 10 μM Ni(II), sufficient to saturate all Ni(II) binding sites, shifts the DNA binding equilibrium to higher NmtR concentrations, decreasing the affinity by ≈100-fold to

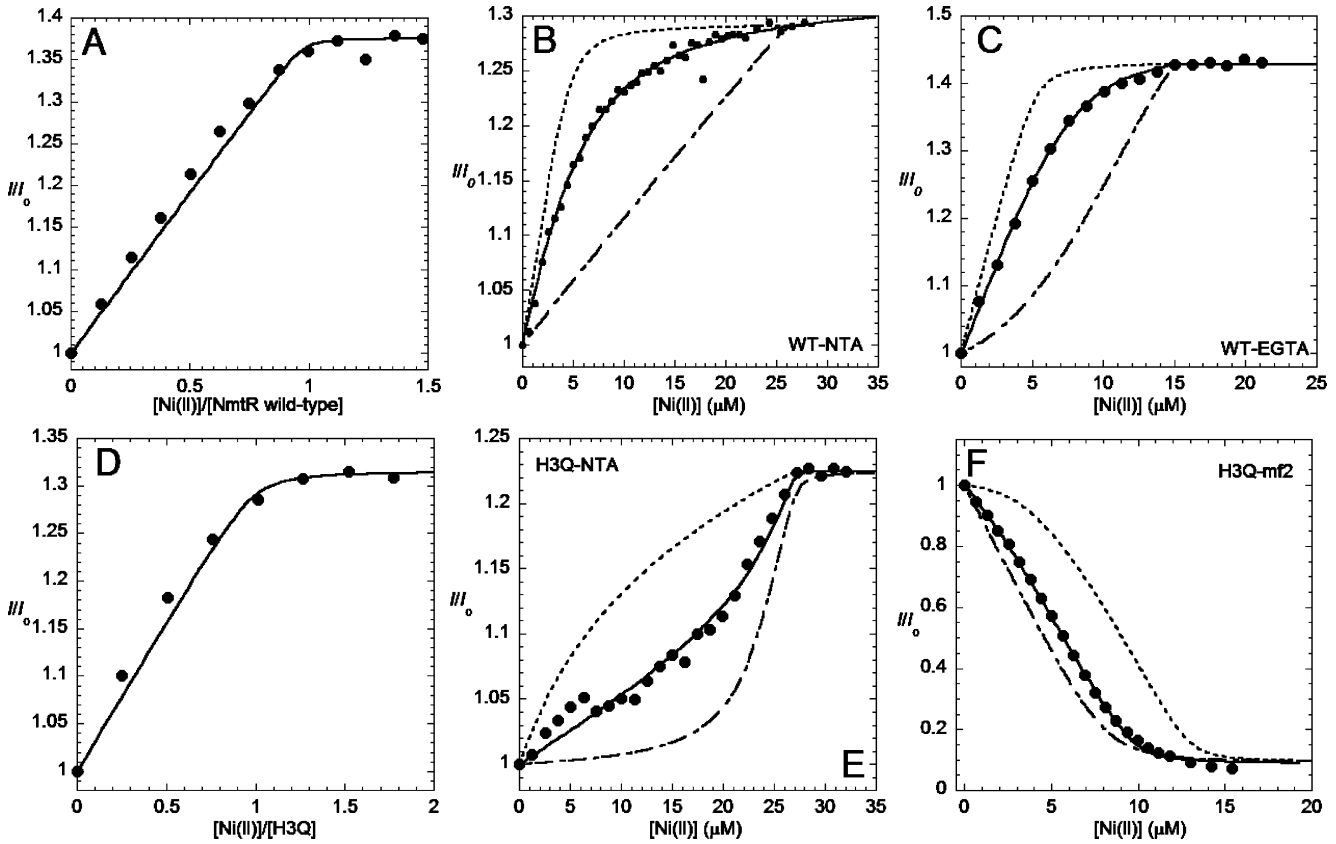

Figure 4. Ni(II) binding to wild-type (A–C) and H3Q (D–F) NmtR at 5.0 μM protein monomer (2.5 μM dimer) in the absence (A and D) or presence of NTA (B and E), EGTA (C), or mf2 (F). Ni(II) binding was monitored by a change in the intrinsic fluorescence intensity (I/I_o) that assumes to be a linear function of Ni(II) occupancy. In the absence of chelator, the red line represents nonlinear least-squares fits to a 1:1 [Ni(II):monomer] binding model. In the presence of chelator, the red line represents nonlinear least-squares fits to a two-step 2:1 Ni(II):dimer binding model defined by K_{Ni1} and K_{Ni2}, with the parameters summarized in Table 1. (A) Wild-type NmtR, $K_{Ni} \geq 8.9 \times 10^8$ M^{-1} (lower limit). (B) Wild-type NmtR (5.0 μM) and NTA (21 μM), $K_{Ni1} = (1.3 \pm 0.2) \times 10^{10}$ M^{-1}, $K_{Ni2} = (0.3 \pm 0.04) \times 10^{10}$ M^{-1}. (C) Wild-type NmtR (5.0 μM) and EGTA (10.0 μM), $K_{Ni1} = (1.1 \pm 0.03) \times 10^{10}$ M^{-1}, $K_{Ni2} = (1.1 \pm 0.03) \times 10^{10}$ M^{-1}. (D) H3Q NmtR, $K_{Ni} \sim 1.50 \times 10^8$ M^{-1} (lower limit). (E) H3Q NmtR (5.0 μM) and NTA (20 μM), $K_{Ni1} = (7.3 \pm 0.8) \times 10^8$ M^{-1}, $K_{Ni2} = (1.0 \pm 0.4) \times 10^8$ M^{-1}. (F) H3Q NmtR (5.0 μM) and mf2 (8.0 μM), $K_{Ni1} = (1.0 \pm 0.5) \times 10^8$ M^{-1}, $K_{Ni2} = (1.0 \pm 0.1) \times 10^7$ M^{-1}. The dashed and dotted–dashed lines represent simulations if K_{Nii} values were 10-fold larger and 10-fold lower than the fitted values, respectively.

Table 1. Ni(II) Binding Affinities of Wild-Type NmtR and Its Mutant Variants[a]

NmtR	K_{Ni1} ($\times 10^{10}$ M^{-1})	K_{Ni2} ($\times 10^{10}$ M^{-1})
wild-type[b]	1.15 ± 0.10	0.70 ± 0.40
H3Q[c]	0.042 ± 0.03	0.001 ± 0.0001
D91Q[d]	0.0120 ± 0.0005	0.001 ± 0.0001
H93Q[d]	0.0031 ± 0.0001	0.001 ± 0.0001
H104Q[d]	0.0004 ± 0.00003	0.001 ± 0.0001
H107Q[d]	0.0034 ± 0.0002	0.001 ± 0.0001
H109Q[b]	0.75 ± 0.25	1.00 ± 0.01
D114Q[b]	0.76 ± 0.04	0.60 ± 0.13
H116Q[b]	0.77 ± 0.18	0.55 ± 0.05
Δ111 NmtR[b]	2.4 ± 1.6	–[e]

[a]Conditions: 10 mM Hepes, pH 7.0, 0.2 M NaCl, 25 °C. [b]Average of K_{Ni} values measured in the presence of NTA or EGTA as a competitor. [c]Average of K_{Ni} values measured in the presence of NTA or mf2 as a competitor. [d]mf2 competition experiments. [e]Not detected, i.e., stoichiometry of one per dimer.

Table 2. Wild-Type NmtR DNA Binding Affinities for Different Metal Complexes[a]

NmtR	Δr_{max}[b]	K_{DNA} ($\times 10^9$ M^{-1})	ΔG_c[c] (kcal mol^{-1})
		I = 0.2	
apo[d]	0.027	28.6 ± 0.4	–
Ni(II)[e]	0.027	1.5 ± 0.1	1.7 ± 0.04
		I = 0.4 and nonspecific competitor[f]	
apo[d]	0.016	9.2 ± 1.0	–
Ni(II)[e]	0.016	0.06 ± 0.01	2.9 ± 0.1
		I = 0.4	
apo[d]	0.020	8.7 ± 1.0	–
Ni(II)[g]	0.020	0.10 ± 0.01	2.7 ± 0.1
Co(II)[g]	0.020	0.21 ± 0.03	2.2 ± 0.1
Zn(II)[g]	0.027	1.5 ± 0.2	1.1 ± 0.1

[a]Conditions: 10 mM Hepes, pH 7.0, 25 °C. [b]Δr_{max} is the maximum change in the fitted anisotropy ($r_{complex} - r_{free}$). [c]$\Delta G_c = -RT \ln(K_{DNA\text{-}Ni}/K_{DNA\text{-}apo})$. [d]For determination of apo K_{DNA}, 500 μM EDTA was added to the binding reaction mixture. [e]For determination of Ni(II) K_{DNA}, 100 μM Ni(II) was added to the binding reaction mixture. [f]Salmon sperm DNA. [g]For determination of metal K_{DNA}, 10 μM Ni(II), Co(II), or Zn(II) was added to the binding reaction mixture.

(8.0 ± 2.0) × 10^7 M^{-1}. The magnitude of this response is defined by the allosteric coupling free energy, ΔG_c,[54] a quantitative measure of the degree to which metal regulates DNA binding. For wild-type NmtR, ΔG_c = 2.8 ± 0.1 kcal

dx.doi.org/10.1021/bi200737a | Biochemistry 2011, 50, 7941–7952

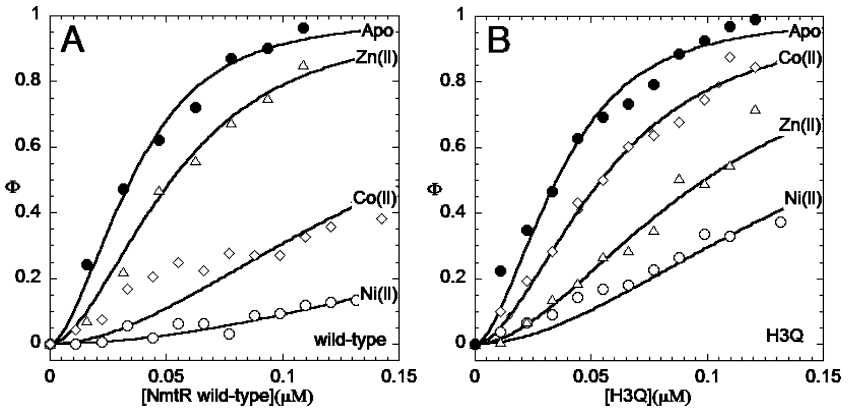

Figure 5. Allosteric negative regulation of DNA binding by various metals for (A) wild-type and (B) H3Q NmtR. Representative data points of binding isotherms depicted with empty and filled symbols for the metal and apo forms, respectively. The lines represent nonlinear least-squares fits to a model in which a dissociable dimer binds to a single DNA. The total anisotropy change is normalized to the apo-NmtR value (Δr_{max}), so for each instance, the anisotropy change observed (Δr_{obs}) is a fraction of that for apo-NmtR. Tables 2 and 3 compile the K_{DNA} values calculated from this analysis, along with values of Δr_{max}: Ni(II) (○), Co(II) (◇), and Zn(II) (△). The data shown for metalated wild-type and H3Q NmtR were acquired in the presence of 10 μM Ni(II), Co(II), or Zn(II).

Table 3. DNA Binding Affinities of H3Q NmtR with Different Metal Complexes[a]

H3Q NmtR	Δr_{max}[b]	K_{DNA} ($\times 10^9$ M^{-1})	ΔG_c[c] (kcal mol^{-1})	wild-type ΔG_c[d] (kcal mol^{-1})
apo[e]	0.019	8.40 ± 1.00	–	–
		10 μM metal[f]		
Ni(II)	0.019	0.07 ± 0.01	2.8 ± 0.1	2.7 ± 0.1
Co(II)	0.019	1.33 ± 0.20	1.1 ± 0.1	2.2 ± 0.1
Zn(II)	0.019	0.35 ± 0.02	2.0 ± 0.1	1.1 ± 0.1

[a]Conditions: 10 mM Hepes, pH 7.0, 0.4 M NaCl, 25 °C. [b]For this NmtR variant, $\Delta r_{max} = 0.019$ ($r_{complex} - r_{free}$). [c]$\Delta G_c = -RT \ln(K_{DNA\text{-}Ni}/K_{DNA\text{-}apo})$. [d]Wild-type NmtR values shown for comparison. [e]For determination of apo K_{DNA}, 500 μM EDTA was added to the binding reaction mixture. [f]For determination of K_{DNA}, 100 μM metal was added to the binding reaction mixture.

mol^{-1}, with the positive sign indicative of negative heterotropic linkage. The specific DNA binding affinity of NmtR is decreased by addition of other metals at a concentration of 10 μM, but the magnitude of the regulation is quantitatively different. Co(II), an inducer of *nmtA* transcription in vivo,[22] is characterized by a ΔG_c of 2.2 ± 0.1 kcal mol^{-1}, which is followed by Zn(II), which reduces the affinity of NmtR for the DNA operator by just ≈6-fold. Zn(II) (10 μM) is sufficient to fully saturate NmtR under these conditions given $K_{Zn} \geq 10^8$ M^{-1};[22] 10 μM Co(II) is approximately 10-fold larger than $1/K_{Co}$ and is thus indicative of ≥90% saturation under these conditions.[22]

His3 Contributes to the Stability of the Metal Complex, and Its Substitution Alters the Rank Order of Allosteric Metal Ions. Some members of the ArsR/SmtB family employ metal ligands from an N-terminal "extension" to coordinate metal to the α3 helix (α3N subfamily),[21] and crystallographic studies suggest that this tail is not likely to be structurally organized.[55] In the N-terminal domain of NmtR, the conserved residue His3 is an excellent candidate for a Ni(II) ligand (Figure 2). This histidine is flanked on each side by Gly, forming a specific sequence (Gly-His-Gly) that can coordinate Ni(II) with one or two deprotonated main chain amides, the α-amino group and/or the side chain histidine Nδ1 or Nε2 atom.[56−60] A bacterial metalloregulator thought to utilize such an arrangement is the Ni(II) efflux regulator *E. coli* RcnR.[26]

The N-terminal residue Met1 is processed during the expression of NmtR as determined by ESI-MS (Table S2 of the Supporting Information), and as a result, little steric clash is expected from the backbone Gly2-His3-Gly4 sequence, in the event of metal coordination. The functional importance of His3 was investigated using a Gln substitution mutant. H3Q NmtR binds Ni(II) with a stoichiometry of 1:1 [Ni(II):protomer] like wild-type NmtR, with a concomitant increase of 30% fluorescence intensity and a lower K_{Ni} limit of $\approx 10^8$ M^{-1} observed from direct titration in the absence of chelator (Figure 4D). However, in the chelator competition experiments, the Ni(II) binding isotherm depicts a shape that is indicative of dramatically decreased affinity with respect to that of wild-type NmtR (Figure 4E,F). The stepwise binding affinities of H3Q NmtR are reduced by ∼20- and ∼700-fold for K_{Ni1} and K_{Ni2}, respectively, relative to those of wild-type NmtR (Table 1). Nevertheless, the DNA binding experiments show that apo H3Q NmtR binds DNA like wild-type NmtR, with a change in anisotropy that is comparable to that of wild-type NmtR (Figure 5B and Table 3). H3Q binding to DNA is still strongly regulated by 10 μM Ni(II), with a ΔG_c^{Ni} of 2.8 kcal mol^{-1} that is the same as that of wild-type NmtR. However, the striking finding is that, in contrast to wild-type NmtR, this mutant is significantly more sensitive to Zn(II)-mediated regulation relative to the cognate metal Co(II). These data reveal that His3 directly influences binding and Ni(II)/Co(II) selectivity of this allosteric switch; additional experiments are required to determine if other features of the N-terminus, e.g., the α-NH_2 group or a main chain amide nitrogen, contribute coordination bonds to the Ni(II)[26] (see Discussion).

Conserved Residues in the α5 Helix Are Essential for Ni(II) Binding Affinity and Allosteric Regulation of DNA Binding. Mutations in the α5 helix of metal sensors CzrA and

SmtB are characterized by loss of function and/or a decrease in Zn(II) binding affinity.[39] NmtR is predicted to coordinate Ni(II) with the four ligands conserved in the α5 helical region relative to the CzrA sequence (D91, H93, H104, and H107) (see Figure 1), and on the basis of Asp-to-Ala and His-to-Arg substitution mutations, all were previously shown to be essential for regulation in an in vivo experiment.[22] Here we substitute each of these residues with a nonliganding and conservative Gln to test the requirement of each for stabilization of the metal complex and allosteric regulation. An increase in the intrinsic Tyr fluorescence in response to Ni(II) binding was not detected for any of these α5 site NmtR variants, suggestive of non-native structure found in each case. Therefore, the fluorescent indicator mf2 was used instead to monitor binding of Ni(II) in competition experiments analogous to an approach used previously.[26,61] Calibration of the affinity of mf2 for Ni(II) using NTA as a competitor gives an affinity $K_{mf2\text{-}Ni}$ of $(2.0 \pm 0.1) \times 10^7$ M^{-1} (Figure S2 of the Supporting Information) that is in reasonable agreement with the previously tabulated affinity $K_{Ni\text{-}Mf2}$ of 7.7×10^6 M^{-1} measured at the same salt concentration.[26,61]

The results of these competition experiments with α5 helix NmtR variants (Figure S2 of the Supporting Information) are indicative of detectable competition with mf2, albeit with a pronounced reduction in K_{Ni1} and K_{Ni2}, in each α5 site variant (Table 1). H104Q NmtR is the most compromised in nickel affinity, with K_{Ni1} decreased by ≥10-fold relative to those of other missense mutants. As described above, the Ni(II)-dependent allosteric regulation of DNA binding was quantified by measuring DNA binding affinity in the absence and presence of 0.1 mM Ni(II), a concentration sufficient to saturate all Ni(II) regulatory sites in each case (Figure S3 of the Supporting Information and Table 4). Surprisingly, the presence of excess metal increases the value of Δr_{max} by 2−3-fold, with the possible exception of that of H104Q NmtR that binds with an affinity and Δr_{max} similar to those of apo wild-type NmtR. These findings are perhaps indicative of a different assembly state on the DNA relative to metal-bound wild-type NmtR. Thus, not only are these mutants refractive to Ni(II)-dependent inhibition of DNA binding, but Ni(II) seems to slightly increase the DNA binding affinity, effectively reversing the sign of ΔG_c if it is analyzed in exactly the same way (Figure S3 of the Supporting Information and Table 4).

Table 4. DNA Binding Affinities of α5 Missense Mutant NmtRs in the Presence of Ni(II)[a]

NmtR		Δr_{max}[b]	K_{DNA} ($\times 10^9$ M^{-1})	ΔG_c[c,d] (kcal mol^{-1})
D91Q	apo[e]	0.026	5.0 ± 0.4	–
	Ni(II)[f]	0.046	7.5 ± 0.1	−0.2 ± 0.1
H93Q	apo[e]	0.019	4.2 ± 0.7	–
	Ni(II)[f]	0.050	16 ± 3.0	−0.8 ± 0.1
H104Q	apo[e]	0.003	0.85 ± 0.22	–
	Ni(II)[f]	0.010	0.77 ± 0.10	−0.1 ± 0.2
H107Q	apo[e]	0.024	50.0 ± 1.0	–
	Ni(II)[f]	0.043	24.0 ± 0.5	0.4 ± 0.01

[a]Conditions: 10 mM Hepes, pH 7.0, 0.4 M NaCl, 25.0 °C. [b]Δr_{max} is the anisotropy change fixed as the maximal response in the fit ($r_{complex} - r_{free}$) to the value for wild-type NmtR. [c]$\Delta G_c = -RT \ln(K_{DNA\text{-}Ni}/K_{DNA\text{-}apo})$. [d]For comparison, $\Delta G_{c,Ni(II)NmtR\ wild\text{-}type} = 2.7 \pm 0.2$ kcal mol^{-1}. [e]For determination of apo K_{DNA}, 500 μM EDTA was added to the binding reaction mixture. [f]For determination of Ni(II) K_{DNA}, 100 μM Ni(II) was added to the binding reaction mixture.

This observation was further explored in H104Q NmtR. The presence of other metals also appears to stabilize formation of the DNA complex, with Ni(II) and Co(II) being the most efficient in increasing the anisotropy of the DNA in a way that is dependent on metal concentration (Figure S4 and Table S3 of the Supporting Information). Interestingly, this binding has residual elements of DNA specificity because an excess of nonspecific DNA reduces the affinity of apo H104Q NmtR by only ≈10-fold when an unrelated DNA probe is used in place of the *nmt* operator (Table S3 of the Supporting Information).

C-Terminal NmtR Gln Substitution Mutants Are Functionally Silent. On the basis of arginine substitution mutants, His109 and His116 were previously reported to be essential for metal-dependent regulation in vivo (Figure 1B).[22] Here we investigate Ni(II) binding affinity and metal-dependent regulation of DNA binding of conservative Gln substitution mutants of H109, D114, H116 and a truncated C-terminal NmtR that is missing residues 112−120 and is designated Δ111 NmtR. For Δ111 NmtR, intrinsic fluorescence experiments conducted in the absence of chelator reveal a metal stoichiometry of just one metal per dimer for Ni(II) and Zn(II), with the second binding event undetected by this method. The change in fluorescence intensity is approximately half that of wild-type NmtR, also consistent with occupancy at one of two sites in the dimer by Ni(II) (Figure 6A).

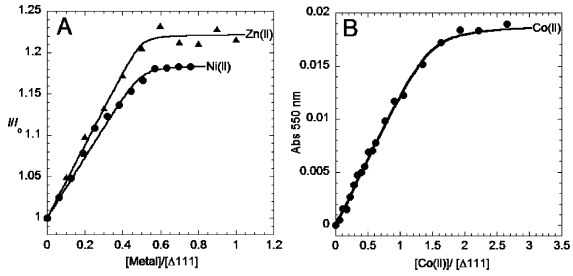

Figure 6. Stoichiometries and affinities of Δ111 NmtR for different metals. (A) Ni(II) (●) and Zn(II) (▲) binding to Δ111 NmtR were monitored by the intrinsic fluorescence intensity change (I/I_o). The lines represent nonlinear least-squares fits to a 0.5:1 ratio (metal:-monomer). $K_{\Delta 111\ NmtR\text{-}Zn(II)} \geq 1.4 \times 10^8$ M^{-1}, and $K_{\Delta 111\ NmtR\text{-}Ni(II)} \geq 9.1 \times 10^7$ M^{-1}; both are lower limits given the stoichiometric nature of these binding isotherms. (B) Co(II) binding was monitored by a change in the visible absorption at 550 nm. The line represents a nonlinear least-squares fit to a 1.5:1 ratio [Co(II):monomer]. $K_{\Delta 111\ NmtR\text{-}Co(II)} \geq 8.4 \times 10^7$ M^{-1}.

Interestingly, Co(II) binding as monitored by UV electronic absorption suggests a stoichiometry of ≈1.4 equiv per monomer (Figure 6B). The shape of these binding curves suggests that Ni(II) and Co(II) bind stoichiometrically to the remaining site(s) under these conditions, with the magnitude of K_{Ni} being very similar to that of wild-type NmtR (Table 1). These results suggest a perturbation of the structural symmetry of the molecule upon deletion of most of the tail despite the fact that this region is flexible in solution (Figure 3).

Apo Δ111 NmtR binds the DNA operator with an affinity comparable to that of wild-type NmtR (Figure 7 and Table 5). However, this mutant is nearly refractive to Ni(II)-mediated regulation, with the coupling free energy decreased to a level comparable to that of noncognate metal Zn(II). Interestingly,

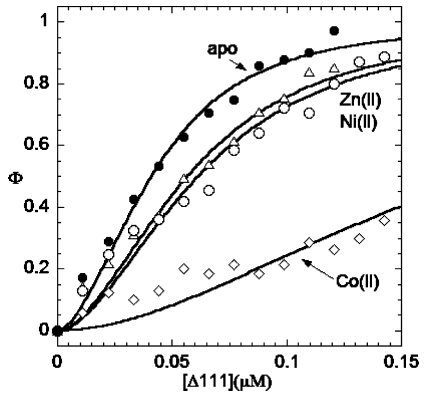

Figure 7. Δ111 NmtR is nearly refractive to Ni(II)-dependent regulation but not to Co(II) regulation. Fluorescence anisotropy experiments were used to monitor DNA binding of the truncated variant. Empty and filled symbols represent data for the metal and apo forms, respectively. The lines represent nonlinear least-squares fits to a model in which a dissociable dimer binds to a single DNA with the parameters listed in Table 5: apoprotein (●), Ni(II) (○), Zn(II) (△), and Co(II) (◇). The experiments were performed in 100 μM metal.

Co(II) is the most potent regulator of Δ111 NmtR, and its effect is indistinguishable from that of Ni(II) regulation of wild-type NmtR (Table 5). One possible explanation of this finding is that the stoichiometry of metal binding may well be a primary determinant of regulation in this mutant rather than the precise identity of the residues in the tail. To test this, we prepared single-Gln substitution mutants H109Q, D114Q, and H116Q. To our surprise, each of the single C-terminal mutant variants binds stoichiometric Ni(II) (Figure S5 of the Supporting Information), and the chelator competition experiments reveal a Ni(II) binding affinity that is indistinguishable from that of wild-type NmtR (Figure S6 of the Supporting Information and Table 1). The Ni(II)-dependent negative allosteric regulation of DNA by these variants is also like that of the wild type at 100 μM added Ni(II) (Figure 8 and Table 6).

UV−Visible Absorption Spectroscopy of Co(II)-Substituted NmtR Variants. The UV−visible absorption spectrum of Co(II)-substituted wild-type NmtR is consistent with a five- or six-coordinate Co(II)-NmtR complex[37,62] (Figure S7A of the Supporting Information). Although all mutant NmtRs bind Co(II) with a stoichiometry of 1.0−1.5 per protomer, the spectrum obtained for each saturated complex differs from that of wild-type NmtR to varying degrees. H3Q NmtR (Figure S7B of the Supporting Information) has a decreased optical absorptivity and is characterized by a spectrum that most closely resembles that of filling of the second site in the wild-type dimer. H109Q NmtR (Figure S7D of the Supporting Information) is also strongly perturbed, with D114Q and H116Q NmtRs (Figure S7E,F of the Supporting Information) most similar to wild-type NmtR. The spectrum of Co(II)-substituted Δ111 NmtR is most strongly perturbed of any mutant, characterized by two maxima at 475 and 570 nm, and a significantly increased molar absorptivity ε_{570} of 140 M^{-1} cm^{-1} (Figure S7C of the Supporting Information); this is suggestive of a reduction in the coordination number for this mutant. It is interesting to note that this Δ111 NmtR is characterized by the strongest Co(II)-dependent regulation of DNA binding of any NmtR (Figure 7, Table 5).

DISCUSSION

The structural basis of metal selectivity by a family of metal sensor proteins, individuals of which respond to distinct metal inducers, is strongly dictated by the detailed structure of the first metal coordination shell and is thus of intrinsic interest.[21,42] In this work, we employ a glutamine scanning mutagenesis approach with the Ni(II) sensor NmtR to investigate cognate Ni(II) versus Co(II) regulation and how the sensing site in NmtR has evolved to functionally discriminate against a highly competitive metal like Zn(II).[42,63] Biochemical and structural studies of α5 prototype Zn(II)-sensing members from the ArsR/SmtB family, e.g., SmtB and CzrA,[36,62] reveal that two Zn(II) bind to a pair of 2-fold symmetric tetrahedral sites that straddle the C-terminal α5 helices of the dimerization domain (Figure 1). Previous studies established a model of metal selectivity based primarily on coordination geometry because binding of the noncognate metal Ni(II) to CzrA to form a non-native octahedral coordination geometry abolishes allosteric negative regulation of protein−DNA interactions. Likewise, Zn(II) is a poorer allosteric regulator of NmtR and was shown to adopt a tetrahedral coordination geometry.[37] In support of this model, evaluation of single-substitution mutants of the zinc sensor CzrA revealed 1:1 correspondence between the ability of a mutant sensor to adopt a nativelike tetrahedral coordination geometry and a near-wild-type allosteric coupling free energy irrespective of metal affinity, K_{Me}.[37] In the cellular milieu, of course, K_{Me} is predicted to have a substantial impact on metal sensing, because this value may well "tune" a sensor to detect changes in metal availability over a physiological range.[42]

In this work, we corroborate and significantly extend previous observations[22] and show that the affinity of NmtR for Ni(II) in its octahedral center[37] is on the order of 10^{10} M^{-1}, a value approximately between that of two other characterized Ni(II) metalloregulators. *E. coli* NikR binds Ni(II) in a square planar geometry, coordinated by three His residues and one Cys with a K_{Ni} of 10^{12} M^{-1},[64] while its functional counterpart, RcnR, is reported to bind Ni(II) with an octahedral geometry with a correspondingly lower affinity of ≈10^{8} M^{-1}.[26] In RcnR, the Ni(II) is modeled to be bound by a Cys and a His at the periphery of what is anticipated to be a four-helix bundle, the side chain of His3, the α-NH_2 group of residue 2, and a main chain amide and a solvent molecule.[26] Co(II), a metal inducer of RcnR in vivo, also adopts an octahedral coordination geometry with Cys as a ligand donor, but this residue is essential for only Co(II) regulation in vivo, not Ni(II).[26] This suggests that although both metals are sensed by RcnR, the functional determinants of the coordination structure may not be identical in each case.

KmtR is the second Ni(II) sensor from the ArsR/SmtB family that is expressed in *Mtb* cytoplasm.[24] KmtR binds Ni(II) with an as yet uncharacterized coordination geometry, although mutagenesis experiments suggest that the Ni(II) is also six-coordinate with a mixture of carboxylate and imidazole ligands.[24] In an experiment designed to estimate the relative affinities of KmtR and NmtR for Ni(II), it was shown that the former has a ≥100-fold higher affinity for Ni(II).[24] Thus, on the basis of the binding affinity reported here for NmtR, KmtR should bind Ni(II) with an affinity of ≥10^{12} M^{-1}. The presence of two regulators in the same cytoplasm makes it possible to sense a metal at distinct concentration ranges (sensitivities) that may allow for a graded metal response.[24] For example, *Mtb*

Table 5. DNA Binding Affinities of Δ111 NmtR Complexed with Various Metal Ions[a]

Δ111 NmtR	Δr_{max}[b]	Δr_{obs}[c]	K_{DNA} ($\times 10^9$ M^{-1})	ΔG_c[d] (kcal mol^{-1})	wild-type ΔG_c[e] (kcal mol^{-1})
apo[f]	0.014	0.013	5.6 ± 1.0	–	
			100 μM metal		
Ni(II)		0.012	1.00 ± 0.02	1.0 ± 0.1	2.7 ± 0.1
Co(II)		0.005	0.12 ± 0.01	2.4 ± 0.1	2.2 ± 0.1
Zn(II)	0.024	0.020	1.20 ± 0.20	0.9 ± 0.1	1.1 ± 0.1

[a]Conditions: 10 mM Hepes, 0.4 M NaCl, 25.0 °C. [b]Δr_{max} is the measured anisotropy maximal response ($r_{complex} - r_{free}$). [c]Δr_{obs} is the observed anisotropy change at the highest protein concentration used in the analysis. [d]$\Delta G_c = -RT \ln(K_{DNA\text{-}Ni}/K_{DNA\text{-}apo})$. [e]Wild-type NmtR values shown for comparison. [f]For determination of apo K_{DNA}, 500 μM EDTA was added to the binding reaction mixture.

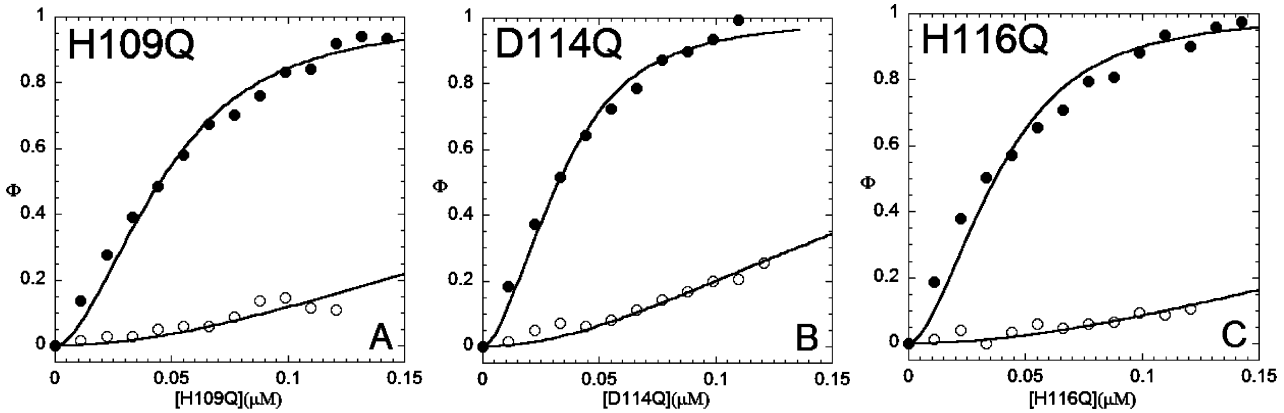

Figure 8. Ni(II)-dependent allosteric regulation of DNA binding by C-terminal NmtR variants (A) H109Q, (B) D114Q, and (C) H116Q. Shown are binding isotherms monitored by a change in the fluorescence anisotropy of the DNA. Titrations conducted in the presence (empty symbols) or absence (filled symbols) of 100 μM Ni(II) are shown. The lines represent nonlinear least-squares fits to a model in which a dissociable dimer binds to a DNA operator. The data are normalized to the maximum anisotropy change (Δr_{max}) that corresponds to apoprotein in each case. Table 6 complies the K_{DNA} values calculated from this analysis, along with Δr_{max} values.

Table 6. DNA Binding Affinities of C-Terminal NmtR Variants[a]

NmtR	Δr_{max}[b]	Δr_{obs}[c]	K_{DNA} ($\times 10^9$ M^{-1})	ΔG_c[d,e] (kcal mol^{-1})
			H109Q	
apo[f]	0.014	0.013	4.3 ± 0.6	–
Ni(II)[g]	0.014[c]	0.001	0.04 ± 0.01	2.8 ± 0.2
			D114Q	
apo[f]	0.020	0.019	10.0 ± 0.2	–
Ni(II)[g]	0.020	0.005	0.08 ± 0.004	3.0 ± 0.03
			H116Q	
apo[f]	0.017	0.017	7.3 ± 0.1	–
Ni(II)[g]	0.017	0.002	0.02 ± 0.002	3.5 ± 0.1

[a]Conditions: 10 mM Hepes, pH 7.0, 0.4 M NaCl, 25.0 °C. [b]Δr_{max} is the measured anisotropy maximal response ($r_{complex} - r_{free}$). [c]Δr_{obs} is the observed anisotropy change at the highest protein concentration used in the analysis. [d]$\Delta G_c = -RT \ln(K_{DNA\text{-}Ni}/K_{DNA\text{-}apo})$. [e]For comparison, $\Delta G_{c,Ni(II)\text{-}NmtR\ wild\text{-}type} = 2.7 \pm 0.2$ kcal mol^{-1}. [f]For determination of apo K_{DNA}, 500 μM EDTA was added to the binding reaction mixture. [g]For determination of Ni(II) K_{DNA}, 100 μM Ni(II) was added to the binding reaction mixture.

encodes two structurally homologous Cu(I) sensors that regulate distinct sets of genes in response to Cu(I) stress at apparently different extracellular Cu(I) regimes.[65,66] It is expected that in vivo derepression will be observed only after Ni(II) concentrations have reached their activation threshold, which for NmtR may be 2−3 orders of magnitude higher than for KmtR.

The allosteric negative heterotropic linkage that characterizes Ni(II)-NmtR ($\Delta G_c \approx 2.8$ kcal mol^{-1}) is of a magnitude similar to that of other ArsR/SmtB members, including the α3N Cd(II) sensor CadC[67] and the α3N Zn(II) site of Cu(I)/Zn(II) sensor BxmR,[68] which recruit one or more ligands from the N-terminal region to coordinate their respective metals. However, this allosteric energy coupling is small relative to that of the paradigm α5 site zinc sensor CzrA ($\Delta G_c \approx 6$ kcal mol^{-1}).[35,39] The origin of this difference is not yet known but strongly suggests that the structural mechanism may well differ between CzrA and NmtR as anticipated on the basis of their distinct metal specificity profile. All of the anticipated metal ligands in the α5 helix are necessary, but not sufficient, for establishing a nativelike metal site structure and metal response profile, and each is required to drive allosteric negative regulation of DNA operator binding. These observations establish a functional difference with the α5 Zn(II)-sensing CzrA, where conservation of just two of the four metal ligands is sufficient for maintenance of a tetrahedral complex and the Zn(II)-mediated allosteric switching mechanism.[39] A novel observation is that the metalated NmtR α5 variants seem to stabilize the formation of higher-order protein−DNA complexes, which may be indicative of metal-mediated stabilization of an allosterically impaired dimeric interface.[69,70]

Our characterization of H3Q NmtR provides strong support for the proposal that His3 in the N-terminus is a direct ligand to the Ni(II) ion because K_{Ni} is greatly decreased in this mutant (Figure 1C). However, provided sufficient Ni(II) is present, H3Q NmtR is characterized by a wild-type ΔG_c. The striking finding is that the primary role of His3 may be to prevent regulation of DNA binding by the noncognate metal Zn(II), because mutagenesis of His3 allows NmtR to recover substantial Zn(II) responsiveness in vitro. H3Q NmtR also exhibits an attenuated Co(II) absorption spectrum and poor

Co(II)-dependent allosteric regulation, consistent with the idea that the Co(II) complex may also be more strongly functionally dependent on His3 for wild-type activity than Ni(II). There is precedent for distinct coordination complexes found by pairs of cognate metals, e.g., Co or Ni in *E. coli* RcnR.[26] On the other hand, Co(II) binds much more weakly than Ni(II) ($K_{Co} \approx 10^6$ M^{-1}) to NmtR,[22] and loss of His3 may simply destabilize the complex to a degree that not all binding sites are saturated at 10 μM Co(II) (Table 3). All we can conclude is that XAS reveals a Ni(II) center in NmtR containing a mixture of histidines and other as yet unidentified N/O ligands.[37] If His3 is indeed a ligand to the Ni(II) ion, this would be a unique structural feature among the ArsR/SmtB family members containing a core α5 metalloregulatory site (Figure 1). Because this N-terminal extension adopts a dynamic, random coil conformation in the absence of Ni(II), it is clearly of sufficient length to reach the C-terminal α5 helix of the opposite protomer.[53] The structure of Zn(II)-bound CzrA suggests that less than 9 Å will separate the residues analogous to Pro14 and His107 in NmtR.[34]

If indeed this is the case, a plausible mechanism of allosteric regulation may involve a reorganization of the N-terminal tail that may be in direct contact with the DNA in the bound apoprotein complex, e.g., Arg8 and Arg10. In fact, in the solution structure of CzrA in complex with DNA, residues in the N-terminus of the α1 helix contact the intervening minor groove of consecutive major grooves that harbor 5′-TGAA recognition elements.[34] Although little structural information is available for members of the α3N family in complex with DNA, other metalloregulators, including *Helicobacter pylori* NikR[71,72] and *H. pylori* Fur,[73,74] possess a flexible N-terminal "arm" that modulates specific DNA interactions.

Our results fail to provide support for the direct involvement of His109 and His116 in the C-terminal tail in metal binding and allosteric regulation, in contrast to the conclusions reached on the basis of the cellular nickel responsiveness of H109R and H116R NmtR;[22] these studies also showed that D114A NmtR exhibited wild-type Ni(II) regulation in vivo. This discrepancy may be attributed to a number of possible explanations, and structural studies will be required to discriminate among them; in any case, they point out the potential shortcomings of assigning function to a residue on the basis of a single substitution. The insertion of a bulky and positively charge arginine residue near the metal binding site could compete for binding of the metal ion (steric inhibition) and/or create an electrostatic repulsive interaction (charge repulsion). Interestingly, such a precedent exists in the case of an arginine substitution mutant of a non-Ni(II) ligand in *E. coli* RcnR that was found to abrogate Ni(II) sensing in vivo.[26] The second possibility is the recruitment of a non-native ligand from multiple available ligand donors, similar to what is believed to happen in other metal sensors SmtB and RcnR.[26,75]

The C-terminal tail is, however, required to maintain a Ni(II) binding stoichiometry of 2:1 as well as a native coordination geometry; indeed, the Δ111 NmtR truncation mutant is characterized by weakened metal-mediated allosteric regulation (ΔG_c = 1 kcal mol^{-1}) relative to that of wild-type NmtR. A Zn(II) sensor CzrA (fCzrA) was previously engineered by the fusion of the N- and C-terminal domains by a flexible peptide interdimeric linker, with the objective of measuring the effects of the perturbations in the dimeric interface on allosteric regulation.[53] In a fCzrA variant where the shortest linker was used and the strongest perturbation in the dimer interface is expected, binding of only one Zn(II) per dimer was detected, analogous to the case for Δ111 NmtR. However, this fCzrA variant is competent with respect to Zn(II) regulation, in contrast to the results shown for Ni(II)-bound Δ111 NmtR. However, this truncation mutant binds Co(II) with four or five ligands and a stoichiometry of up to three metals per dimer, which efficiently negatively regulates DNA binding (ΔG_c = 2.4 kcal mol^{-1}) to an extent similar to that observed for the Co(II) complex of wild-type NmtR.

These data taken collectively suggest the C-terminal tail functions indirectly in Ni(II) and Co(II) sensing by NmtR and effectively controls the stoichiometry and coordination geometry of the Ni(II) and Co(II) complexes to varying degrees; it is unlikely, however, to form a coordination bond to the regulatory Ni(II). This conclusion is consistent with the sequence alignment. Indeed, the tail appears to be essential for Ni(II) regulation, but less so for Co(II) regulation. The regulatory Ni(II) complex in NmtR is characterized by features of an N-terminal Ni(II)-binding motif that may be structurally similar to the "nickel hook" motif in Ni(II) superoxide dismutase (SodN)[58] and inferred from the mutagenesis studies of *E. coli* RcnR.[26] High-resolution structural studies are required to provide further support for what may be a unique metalloregulatory model in ArsR/SmtB family sensors.[21,23]

■ ASSOCIATED CONTENT

Ⓢ Supporting Information

Supplementary Tables S1−S3 and supplementary Figures S1−S7. This material is available free of charge via the Internet at http://pubs.acs.org.

■ AUTHOR INFORMATION

Corresponding Author

*Department of Chemistry, Indiana University, 212 S. Hawthorne Dr., Bloomington, IN 47405-7102. E-mail: giedroc@indiana.edu. Telephone: (812) 856-3178. Fax: (812) 856-5710.

Funding

This work was supported by National Institutes of Health Grant GM042569 to D.P.G.

■ ACKNOWLEDGMENTS

This work has been submitted by H.R.-C. to Texas A&M University in partial fulfillment of the requirements for a Ph.D. in Biochemistry.

■ ABBREVIATIONS

ArsR, arsenic repressor; CsoR, copper-sensitive operon repressor; CzrA, chromosomally encoded zinc-regulated repressor; *Mtb*, *Mycobacterium tuberculosis*; EGTA, *N*,*N*′-ethylene glycol tetraacetic acid; Fur, iron uptake regulator; mf2, mag-fura 2; NikR, nickel-responsive regulator of the *nik* operon; NmtR, nickel-dependent *Mtb* repressor; NTA, nitrilotriacetic acid; Nur, nickel uptake regulator; PEI, polyethylenimine; RcnR, resistance to cobalt and nickel repressor; SmtB, *Synechococcus* metallothionein.

■ REFERENCES

(1) Cole, S. T., Brosch, R., Parkhill, J., Garnier, T., Churcher, C., Harris, D., Gordon, S. V., Eiglmeier, K., Gas, S., Barry, C. E. III, Tekaia, F., Badcock, K., Basham, D., Brown, D., Chillingworth, T., Connor, R., Davies, R., Devlin, K., Feltwell, T., Gentles, S., Hamlin, N., Holroyd, S.,

Hornsby, T., Jagels, K., Krogh, A., McLean, J., Moule, S., Murphy, L., Oliver, K., Osborne, J., Quail, M. A., Rajandream, M. A., Rogers, J., Rutter, S., Seeger, K., Skelton, J., Squares, R., Squares, S., Sulston, J. E., Taylor, K., Whitehead, S., and Barrell, B. G. (1998) Deciphering the biology of *Mycobacterium tuberculosis* from the complete genome sequence. *Nature 393*, 537−544.

(2) Agranoff, D., and Krishna, S. (2004) Metal ion transport and regulation in *Mycobacterium tuberculosis*. *Front. Biosci. 9*, 2996−3006.

(3) Brosch, R., Gordon, S. V., Eiglmeier, K., Garnier, T., Tekaia, F., Yeramian, E., and Cole, S. T. (2000) Genomics, Biology, and Evolution of the *Mycobacterium tuberculosis* Complex. In *Molecular Genetics of Mycobacteria* (Hatfull, G. F., and Jacobs, W. R., Jr., Eds.) pp 19−36, American Society for Microbiology Press, Washington, DC.

(4) Weinberg, E. D. (2009) Iron availability and infection. *Biochim. Biophys. Acta 1790*, 600−605.

(5) Kehl-Fie, T. E., and Skaar, E. P. (2010) Nutritional immunity beyond iron: A role for manganese and zinc. *Curr. Opin. Chem. Biol. 14*, 218−224.

(6) Mulrooney, S. B., and Hausinger, R. P. (2003) Nickel uptake and utilization by microorganisms. *FEMS Microbiol. Rev. 27*, 239−261.

(7) Doukov, T. I., Iverson, T. M., Seravalli, J., Ragsdale, S. W., and Drennan, C. L. (2002) A Ni-Fe-Cu center in a bifunctional carbon monoxide dehydrogenase/acetyl-CoA synthase. *Science 298*, 567−572.

(8) Sukdeo, N., Clugston, S. L., Daub, E., and Honek, J. F. (2004) Distinct classes of glyoxalase I: Metal specificity of the *Yersinia pestis*, *Pseudomonas aeruginosa*, and *Neisseria meningitidis* enzymes. *Biochem. J. 384*, 111−117.

(9) Smith, N. H., Gordon, S. V., de laRua-Domenech, R., Clifton-Hadley, R. S., and Hewinson, R. G. (2006) Bottlenecks and broomsticks: The molecular evolution of *Mycobacterium bovis*. *Nat. Rev. Microbiol. 4*, 670−681.

(10) Clemens, D. L., Lee, B. Y., and Horwitz, M. A. (1995) Purification, characterization, and genetic analysis of *Mycobacterium tuberculosis* urease, a potentially critical determinant of host-pathogen interaction. *J. Bacteriol. 177*, 5644−5652.

(11) Sendide, K., Deghmane, A.-E., Reyrat, J.-M., Talal, A., and Hmama, Z. (2004) *Mycobacterium bovis* BCG Urease Attenuates Major Histocompatibility Complex Class II Trafficking to the Macrophage Cell Surface. *Infect. Immun. 72*, 4200−4209.

(12) Baena, A., and Porcelli, S. A. (2009) Evasion and subversion of antigen presentation by *Mycobacterium tuberculosis*. *Tissue Antigens 74*, 189−204.

(13) Yokoi, K., Uthus, E. O., and Nielsen, F. H. (2003) Nickel deficiency diminishes sperm quantity and movement in rats. *Biol. Trace Elem. Res. 93*, 141−154.

(14) Denkhaus, E., and Salnikow, K. (2002) Nickel essentiality, toxicity, and carcinogenicity. *Crit. Rev. Oncol. Hematol. 42*, 35−56.

(15) Nielsen, F.H. (1991) Nutritional requirements for boron, silicon, vanadium, nickel, and arsenic: Current knowledge and speculation. *FASEB J. 5*, 2661−2667.

(16) Nielsen, F. H. (1993) Ultratrace elements of possible importance for human health: An update. *Prog. Clin. Biol. Res. 380*, 355−376.

(17) Agranoff, D. D., and Krishna, S. (1998) Metal ion homeostasis and intracellular parasitism. *Mol. Microbiol. 28*, 403−412.

(18) Rodriguez, G. M., and Smith, I. (2003) Mechanisms of iron regulation in mycobacteria: Role in physiology and virulence. *Mol. Microbiol. 47*, 1485−1494.

(19) Wagner, D., Maser, J., Moric, I., Boechat, N., Vogt, S., Gicquel, B., Lai, B., Reyrat, J.-M., and Bermudez, L. (2005) Changes of the phagosomal elemental concentrations by *Mycobacterium tuberculosis* Mramp. *Microbiology 151*, 323−332.

(20) Wagner, D., Maser, J., Lai, B., Cai, Z., Barry, C. E. III, Honer zu Bentrup, K., Russell, D. G., and Bermudez, L. E. (2005) Elemental Analysis of *Mycobacterium avium*-, *Mycobacterium tuberculosis*-, and *Mycobacterium smegmatis*-containing Phagosomes Indicates Pathogen-Induced Microenvironments within the Host Cell's Endosomal System. *J. Immunol. 174*, 1491−1500.

(21) Ma, Z., Jacobsen, F. E., and Giedroc, D. P. (2009) Coordination Chemistry of Bacterial Metal Transport and Sensing. *Chem. Rev. 109*, 4644−4681.

(22) Cavet, J. S., Meng, W., Pennella, M. A., Appelhoff, R. J., Giedroc, D. P., and Robinson, N. J. (2002) A nickel-cobalt-sensing ArsR-SmtB family repressor. Contributions of cytosol and effector binding sites to metal selectivity. *J. Biol. Chem. 277*, 38441−38448.

(23) Osman, D., and Cavet, J. S. (2010) Bacterial metal-sensing proteins exemplified by ArsR-SmtB family repressors. *Nat. Prod. Rep. 27*, 668−680.

(24) Campbell, D. R., Chapman, K. E., Waldron, K. J., Tottey, S., Kendall, S., Cavallaro, G., Andreini, C., Hinds, J., Stoker, N. G., Robinson, N. J., and Cavet, J. S. (2007) Mycobacterial Cells Have Dual Nickel-Cobalt Sensors. *J. Biol. Chem. 282*, 32298−32310.

(25) Rodrigue, A., Effantin, G., and Mandrand-Berthelot, M.-A. (2005) Identification of *rcnA*(*yohM*), a Nickel and Cobalt Resistance Gene in *Escherichia coli*. *J. Bacteriol. 187*, 2912−2916.

(26) Iwig, J. S., Leitch, S., Herbst, R. W., Maroney, M. J., and Chivers, P. T. (2008) Ni(II) and Co(II) Sensing by *Escherichia coli* RcnR. *J. Am. Chem. Soc. 130*, 7592−7606.

(27) Iwig, J. S., Rowe, J. L., and Chivers, P. T. (2006) Nickel homeostasis in *Escherichia coli*: The *rcnR-rcnA* efflux pathway and its linkage to NikR function. *Mol. Microbiol. 62*, 252−262.

(28) Liu, T., Ramesh, A., Ma, Z., Ward, S. K., Zhang, L. M., George, G. N., Talaat, A. M., Sacchettini, J. C., and Giedroc, D. P. (2007) CsoR is a novel *Mycobacterium tuberculosis* copper-sensing transcriptional regulator. *Nat. Chem. Biol. 3*, 60−68.

(29) De Pina, K., Desjardin, V., Mandrand-Berthelot, M.-A., Giordano, G., and Wu, L.-F. (1999) Isolation and Characterization of the *nikR* Gene Encoding a Nickel-Responsive Regulator in *Escherichia coli*. *J. Bacteriol. 181*, 670−674.

(30) Chivers, P. T., and Sauer, R. T. (2000) Regulation of high affinity nickel uptake in bacteria. Ni^{2+}-dependent interaction of NikR with wild-type and mutant operator sites. *J. Biol. Chem. 275*, 19735−19741.

(31) Schreiter, E. R., Wang, S. C., Zamble, D. B., and Drennan, C. L. (2006) NikR-operator complex structure and the mechanism of repressor activation by metal ions. *Proc. Natl. Acad. Sci. U.S.A. 103*, 13676−13681.

(32) Ahn, B.-E., Cha, J., Lee, E.-J., Han, A.-R., Thompson, C. J., and Roe, J.-H. (2006) Nur, a nickel-responsive regulator of the Fur family, regulates superoxide dismutases and nickel transport in *Streptomyces coelicolor*. *Mol. Microbiol. 59*, 1848−1858.

(33) An, Y. J., Ahn, B. E., Han, A. R., Kim, H. M., Chung, K. M., Shin, J. H., Cho, Y. B., Roe, J. H., and Cha, S. S. (2009) Structural basis for the specialization of Nur, a nickel-specific Fur homolog, in metal sensing and DNA recognition. *Nucleic Acids Res. 37*, 3442−3451.

(34) Arunkumar, A. I., Campanello, G. C., and Giedroc, D. P. (2009) Solution structure of a paradigm ArsR family zinc sensor in the DNA-bound state. *Proc. Natl. Acad. Sci. U.S.A. 106*, 18177−18182.

(35) Grossoehme, N. E., and Giedroc, D. P. (2009) Energetics of allosteric negative coupling in the zinc sensor *S. aureus* CzrA. *J. Am. Chem. Soc. 131*, 17860−17870.

(36) Eicken, C., Pennella, M. A., Chen, X., Koshlap, K. M., VanZile, M. L., Sacchettini, J. C., and Giedroc, D. P. (2003) A metal-ligand-mediated intersubunit allosteric switch in related SmtB/ArsR zinc sensor proteins. *J. Mol. Biol. 333*, 683−695.

(37) Pennella, M. A., Shokes, J. E., Cosper, N. J., Scott, R. A., and Giedroc, D. P. (2003) Structural elements of metal selectivity in metal sensor proteins. *Proc. Natl. Acad. Sci. U.S.A. 100*, 3713−3718.

(38) Kuppuraj, G., Dudev, M., and Lim, C. (2009) Factors Governing Metal-Ligand Distances and Coordination Geometries of Metal Complexes. *J. Phys. Chem. B 113*, 2952−2960.

(39) Pennella, M. A., Arunkumar, A. I., and Giedroc, D. P. (2006) Individual metal ligands play distinct functional roles in the zinc sensor *Staphylococcus aureus* CzrA. *J. Mol. Biol. 356*, 1124−1136.

(40) Waldron, K. J., and Robinson, N. J. (2009) How do bacterial cells ensure that metalloproteins get the correct metal? *Nat. Rev. Microbiol. 7*, 25−35.

(41) Chen, P. R., and He, C. (2008) Selective recognition of metal ions by metalloregulatory proteins. *Curr. Opin. Chem. Biol. 12*, 214–221.
(42) Reyes-Caballero, H., Campanello, G. C., and Giedroc, D. P. (2011) Metalloregulatory proteins: Metal selectivity and allosteric switching. *Biophys. Chem. 156*, 103–114.
(43) Reyes-Caballero, H., Guerra, A. J., Jacobsen, F. E., Kazmierczak, K. M., Cowart, D., Koppolu, U. M. K., Scott, R. A., Winkler, M. E., and Giedroc, D. P. (2010) The Metalloregulatory Zinc Site in *Streptococcus pneumoniae* AdcR, a Zinc-activated MarR Family Repressor. *J. Mol. Biol. 403*, 197–216.
(44) Kuzmic, P. (1996) Program DYNAFIT for the analysis of enzyme kinetic data: Application to HIV proteinase. *Anal. Biochem. 237*, 260–273.
(45) Delaglio, F., Grzesiek, S., Vuister, G. W., Zhu, G., Pfeifer, J., and Bax, A. (1995) NMRPipe: A multidimensional spectral processing system based on UNIX pipes. *J. Biomol. NMR 6*, 277–293.
(46) Johnson, B. A., and Blevins, R. A. (1994) NMR View: A computer program for the visualization and analysis of NMR data. *J. Biomol. NMR 5*, 603–614.
(47) Grzesiek, S., and Bax, A. (1992) Improved 3D triple-resonance NMR techniques applied to a 31 kDa protein. *J. Magn. Reson. 96*, 432–440.
(48) Bax, A., and Ikura, M. (1991) An efficient 3D NMR technique for correlating the proton and ^{15}N backbone amide resonances with the α-carbon of the preceding residue in uniformly $^{15}N/^{13}C$ enriched proteins. *J. Biomol. NMR 1*, 99–104.
(49) Wittekind, M., and Mueller, L. (1993) HNCACB, a high-sensititity 3D NMR experiment to correlate amide-proton and nitrogen resonances with the α- and β-carbon resonaces in proteins. *J. Magn. Reson. 101*, 201–205.
(50) Shen, Y., Delaglio, F., Cornilescu, G., and Bax, A. (2009) TALOS+: A hybrid method for predicting protein backbone torsion angles from NMR chemical shifts. *J. Biomol. NMR 44*, 213–223.
(51) Perrin, D. D., and Dempsey, B. (1979) *Buffers for pH and Metal Ion Control*, 2nd ed., Chapman and Hall, New York.
(52) Martell, A. E., and Smith, R. M., Eds. (2003) NIST Standard Reference Database 46, version 8.0, National Institute of Standards and Technology, Gaithersburg, MD.
(53) Lee, S., Arunkumar, A. I., Chen, X., and Giedroc, D. P. (2006) Structural Insights into Homo- and Heterotropic Allosteric Coupling in the Zinc Sensor *S. aureus* CzrA from Covalently Fused Dimers. *J. Am. Chem. Soc. 128*, 1937–1947.
(54) Giedroc, D. P., and Arunkumar, A. I. (2007) Metal sensor proteins: Nature's metalloregulated allosteric switches. *Dalton Trans. 7*, 3107–3120.
(55) Ye, J., Kandegedara, A., Martin, P., and Rosen, B. P. (2005) Crystal Structure of the *Staphylococcus aureus* pI258 CadC Cd(II)/Pb(II)/Zn(II)-Responsive Repressor. *J. Bacteriol. 187*, 4214–4221.
(56) Farkas, E., Sovago, I., and Gergely, A. (1983) Studies on transition-metal peptide complexes. 8. Parent and mixed-ligands complexes of histidine-containing dipeptides. *J. Chem. Soc., Dalton Trans.*, 1545–1551.
(57) Sovago, I., and Osz, K. (2006) Metal ion selectivity of oligopeptides. *Dalton Trans.*, 3841–3854.
(58) Barondeau, D. P., Kassmann, C. J., Bruns, C. K., Tainer, J. A., and Getzoff, E. D. (2004) Nickel Superoxide Dismutase Structure and Mechanism. *Biochemistry 43*, 8038–8047.
(59) Herbst, R.W., Guce, A., Bryngelson, P. A., Higgins, K. A., Ryan, K. C., Cabelli, D. E., Garman, S. C., and Maroney, M. J. (2009) Role of conserved tyrosine residues in NiSOD catalysis: A case of convergent evolution. *Biochemistry 48*, 3354–3369.
(60) Ryan, K. C., Johnson, O. E., Cabelli, D. E., Brunold, T. C., and Maroney, M. J. (2010) Nickel superoxide dismutase: Structural and functional roles of Cys2 and Cys6. *J. Biol. Inorg. Chem. 15*, 795–807.
(61) Golynskiy, M. V., Gunderson, W. A., Hendrich, M. P., and Cohen, S. M. (2006) Metal binding studies and EPR spectroscopy of the manganese transport regulator MntR. *Biochemistry 45*, 15359–15372.
(62) VanZile, M. L., Chen, X., and Giedroc, D. P. (2002) Structural characterization of distinct α3N and α5 metal sites in the cyanobacterial zinc sensor SmtB. *Biochemistry 41*, 9765–9775.
(63) Waldron, K. J., Rutherford, J. C., Ford, D., and Robinson, N. J. (2009) Metalloproteins and metal sensing. *Nature 460*, 823–830.
(64) Wang, S. C., Dias, A. V., and Zamble, D. B. (2009) The "metallo-specific" response of proteins: A perspective based on the *Escherichia coli* transcriptional regulator NikR. *Dalton Trans.*, 2459–2466.
(65) Ward, S. K., Hoye, E. A., and Talaat, A. M. (2008) The global responses of *Mycobacterium tuberculosis* to physiological levels of copper. *J. Bacteriol. 190*, 2939–2946.
(66) Festa, R. A., Jones, M. B., Butler-Wu, S., Sinsimer, D., Gerads, R., Bishai, W. R., Peterson, S. N., and Darwin, K. H. (2011) A novel copper-responsive regulon in *Mycobacterium tuberculosis*. *Mol. Microbiol. 79*, 133–148.
(67) Busenlehner, L. S., Weng, T. C., Penner-Hahn, J. E., and Giedroc, D. P. (2002) Elucidation of primary(α3N) and vestigial(α5) heavy metal-binding sites in *Staphylococcus aureus* pI258 CadC: Evolutionary implications for metal ion selectivity of ArsR/SmtB metal sensor proteins. *J. Mol. Biol. 319*, 685–701.
(68) Liu, T., Chen, X. H., Ma, Z., Shokes, J., Hemmingsen, L., Scott, R. A., and Giedroc, D. P. (2008) A Cu^{I}-sensing ArsR family metal sensor protein with a relaxed metal selectivity profile. *Biochemistry 47*, 10564–10575.
(69) Salgado, E. N., Ambroggio, X. I., Brodin, J. D., Lewis, R. A., Kuhlman, B., and Tezcan, F. A. (2009) Metal templated design of protein interfaces. *Proc. Natl. Acad. Sci. U.S.A. 107*, 1827–1832.
(70) Brodin, J. D., Medina-Morales, A., Ni, T., Salgado, E. N., Ambroggio, X. I., and Tezcan, F. A. (2010) Evolution of Metal Selectivity in Templated Protein Interfaces. *J. Am. Chem. Soc. 132*, 8610–8617.
(71) Benanti, E. L., and Chivers, P. T. (2007) The N-terminal arm of the *Helicobacter pylori* Ni^{2+}-dependent transcription factor NikR is required for specific DNA binding. *J. Biol. Chem. 282*, 20365–20375.
(72) Benanti, E. L., and Chivers, P. T. (2010) *Geobacter uraniireducens* NikR Displays a DNA Binding Mode Distinct from Other Members of the NikR Family. *J. Bacteriol. 192*, 4327–4336.
(73) Dian, C., Vitale, S., Leonard, G. A., Bahlawane, C., Fauquant, C., Leduc, D., Muller, C., de Reuse, H., Michaud-Soret, I., and Terradot, L. (2011) The structure of the *Helicobacter pylori* ferric uptake regulator Fur reveals three functional metal binding sites. *Mol. Microbiol. 79*, 1260–1275.
(74) Choi, S. S., Chivers, P. T., and Berg, D. E. (2011) Point mutations in *Helicobacter pylori*'s fur regulatory gene that alter resistance to metronidazole, a prodrug activated by chemical reduction. *PLoS One 6*, e18236.
(75) VanZile, M. L., Cosper, N. J., Scott, R. A., and Giedroc, D. P. (2000) The zinc metalloregulatory protein *Synechococcus* PCC7942 SmtB binds a single zinc ion per monomer with high affinity in a tetrahedral coordination geometry. *Biochemistry 39*, 11818–11829.